Evaluation of Pile Stress Based on Response Displacement Method Considering Earth Pressure and Sidewall Friction Acting on Embedded Footing

- Case of Dry Sand Layer on Liquefied Soil -

Shuji TAMURA
Disaster Prevention Research Institute, Kyoto University, Japan

Takenori HIDA
Tokyo University of Science, Japan

SUMMARY:
A response displacement method with earth pressure and sidewall friction acting on an embedded footing has been developed. Dynamic centrifuge tests on a superstructure-footing model that was supported by 2×2 piles in a sand deposit, a dry sand layer on liquefied soil, were conducted to verify the effectiveness of the proposed method. The following conclusions were drawn. (1) Estimated amplitudes of the resultant force of the earth pressure and sidewall friction and the estimated phase difference between the resultant force and the structure inertia force showed good agreement with the experimentally obtained results. (2) Estimated amplitudes of the bending moment at the pile head and the shear force at the pile tip agreed well with the observed results. To estimate the shear force at the pile tip, not only the embedment effects but also accurate subgrade reaction coefficients are necessary.

Keywords: Seismic deformation method, Soil liquefaction, Pile stress, Seismic earth pressure, Embedment effect

1. INTRODUCTION

Seismic earth pressure and sidewall friction acting on an embedded footing have effects on pile stress (Sugimura et al., 1984; Fujii et al., 1998). Therefore, the embedment effects of the footing, the amplitude of the resultant force of earth pressure and sidewall friction, and the phase difference between the resultant force and the structure inertia force are important for the seismic design of pile foundations in conformity to their performance.

Garde and Dobry (1998) reported that the contribution of the passive side accounts for more than half to the total capacity of an embedded footing based on cyclic lateral loading centrifuge tests with relative density of D_r=75%. Tamura et al. (2007) demonstrated that the total earth pressure in the dense sand case plays an important role in reducing the shear force at pile heads based on dynamic centrifuge tests in a superstructure-footing model supported by piles in sand deposits of different relative densities of D_r=45%, 75% and 95%. Tamura et al. (2005) also reported that the phase difference between a structural inertia force and total earth pressure can be estimated by considering the natural period of the superstructure, the predominant period of the ground, the ground displacement, and the footing displacement. However, estimating pile stress with the embedment effects remains difficult.

The objectives of this study are: 1) to estimate the amplitudes of the earth pressure and sidewall friction acting on an embedded footing supported by pile foundation during an earthquake, 2) to estimate the phase difference between the structure inertial force and the resultant force of earth pressure and sidewall friction, and 3) to evaluate the bending moment and shear force of a pile considering the earth pressure and sidewall friction. For this purpose, a response displacement method with earth pressure and sidewall friction has been developed. To verify the effectiveness of the proposed method, dynamic centrifuge tests were conducted on a superstructure-footing model that was supported by 2×2 piles in a sand deposit, a dry sand layer on liquefied soil.

2. CENTRIFUGE TESTS

2.1 Test Cases

Six dynamic centrifuge tests were performed with centrifugal acceleration of 40 × *g* using the geotechnical centrifuge at the Disaster Prevention Research Institute, Kyoto University. A pile-footing-superstructure model was prepared in a laminar shear box with inner dimensions of 450 mm (length) × 150 mm (width) × 200 mm (height). Table 1 presents all test cases in which the piles' bending stiffness, the natural period of a superstructure, and the soil relative density were varied.

2.2 Test Model

2×2 pile models of two types were used for the tests. Table 2 presents the pile conditions. The high stiffness pile was modeled with an 8-mm-diameter round stainless steel bar. The bending stiffness, *EI* of the pile model was 3.85 × 105 Ncm^2. The low stiffness pile was modeled with an 8-mm-diameter round aluminum pipe. The bending stiffness, *EI* of the pile model was 0.84 × 105 Ncm^2, which is 22% of the high stiffness pile model. Figure 1 presents the model setup and sensor location. The lid-shaped footing was modeled with rigid brass of 90 mm (shaking direction) × 68 mm (width) × 55 mm (height). The pile heads were linked rigidly to the upper plate of the footing. Their tips were also linked rigidly to the laminar shear box. The strain gauges at the pile heads were not in contact with the soil. Four plates supported by small load cells were set up on the active and passive sides and shearing sides of the footing. The resultant force of the earth pressure and sidewall friction is defined as the sum of the earth pressure acting on the active and passive sides of the footing and the shearing forces acting on the footing's sidewalls parallel to the shaking direction. The baseline of the earth pressure and wall friction amplitudes were set to zero before the centrifuge test. Toyoura sand was pasted on active and passive sides and on shearing sides of the footing models to increase friction between the footing surface and the soil. The footing was embedded 44 mm into the dry sand before the test.

The natural period of the superstructure in Cases 1, 2, 5, and 6, supported by plate springs under the fixed footing condition was 0.0075 s. The natural period of the superstructure in Cases 3 and 4, sup-

Table 1. Test cases

	Case 1	Case 2	Case 3	Case 4	Case 5	Case 6
Piles' bending stiffness	High	Low	High	Low	High	Low
Natural period of superstructure	0.0075 s (0.3s)		0.125 s (5.0 s)		0.0075 s (0.3s)	
Relative density of soil model	30%				80%	

(Prototype scale)

Table 2. Pile condition

	Pile with high bending stiffness	Pile with low bending stiffness
Pile materials	Stainless steel bar	Aluminum pipe
Diameter, Thickness (Prototype scale)	ϕ=8mm (ϕ=32cm)	ϕ=8mm, t=0.8mm (ϕ=32cm,t=3.2cm)
Bending stiffness (Prototype scale)	3.85 × 10^5 Ncm^2 (9.86 × 10^4 kNm^2)	0.84 × 10^5 Ncm^2 (2.14 × 10^4 kNm^2)

(Prototype scale)

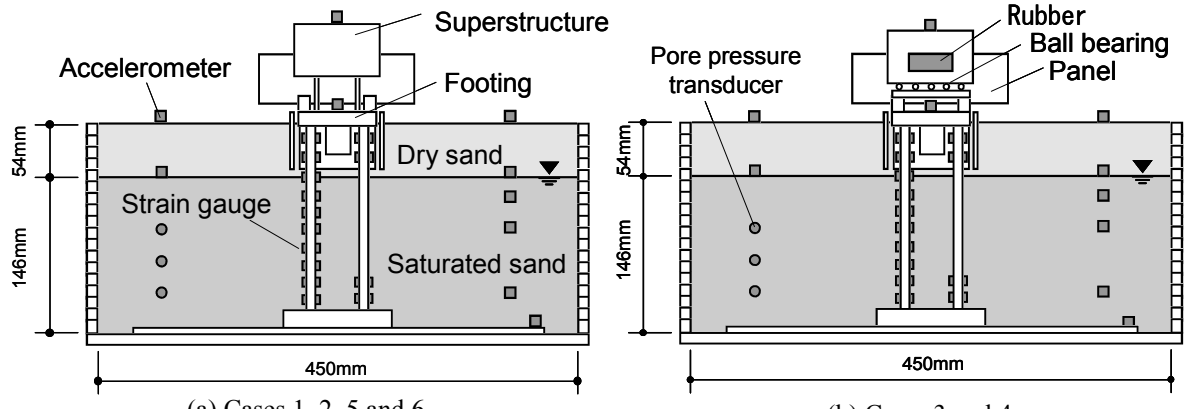

(a) Cases 1, 2, 5 and 6

(b) Cases 3 and 4

Figure 1. Model setup and sensor locations

ported by ball bearings, was 0.125 s, which was adjusted by rubber sheets between the superstructure and the panel fixed on the footing. The respective masses of the superstructure and footing were 2.0 kg and 0.99 kg.

Dry sand was air-pluviated to prepare a uniform soil layer with relative density D_r of 30% in Cases 1–4 and 80% in Cases 5 and 6. Toyoura sand (D_{50}=0.21 mm) was used. The water table was set to 54 mm below the ground surface for all tests. Excitation for the test used Hachinohe 1968 NS. The peak acceleration was scaled to about 3 m/s^2 in prototype scale. In addition to the earth pressure and the sidewall friction acting on the footing, the horizontal accelerations of the superstructure, the footing, the soil and the shear box base, and the excess pore water pressure were measured. All data presented in the following sections are of prototype scale.

3. CENTRIFUGE TEST RESULTS

3.1 Forces acting on footing and pile stress for Cases 1 and 3

Figures 2 and 3 depict the time histories of forces acting on the footing, the pile stresses, and the excess pore water pressure ratios at GL-4.16 m and GL-6.56 m for Cases 1 and 3, respectively. These include the structural inertia, which is the sum of the superstructure and footing inertia forces, the resultant force of the earth pressure and sidewall friction acting on the embedded footing, the sum of the shear forces at the pile heads and the average bending moment at the pile heads. The earth pressure and the sidewall friction were measured directly using the load cells. The excess pore water pressure ratio reached 1 at about 20 s after the shaking. The structural inertia amplitude in Case 3 was extremely small because the superstructure inertia and the footing inertia tended to be out of phase by 180 deg. The resultant force of earth pressure and sidewall friction, the shear force, and the bending moment at the pile head increased rapidly with the progress of liquefaction. The waveforms of the shear force and the bending moment did not resemble that of the structure inertia, but they were similar to that of the resultant force of earth pressure and sidewall friction for both cases, which indicates that the shear force and the bending moment were caused mainly by the earth pressure and the sidewall friction.

3.2 Relation between Structure Inertia and the Resultant Force of Earth Pressure and Sidewall Friction

Figure 4 portrays the relation between the structure inertia and the resultant force of the earth pressure

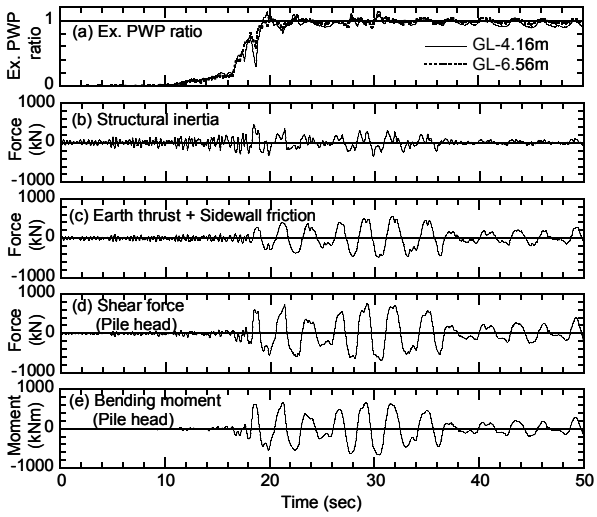

Figure 2. Excess pore water pressure ratio, structural inertia, resultant force of earth pressure and sidewall friction, shear force and bending moment at pile head (Case 1)

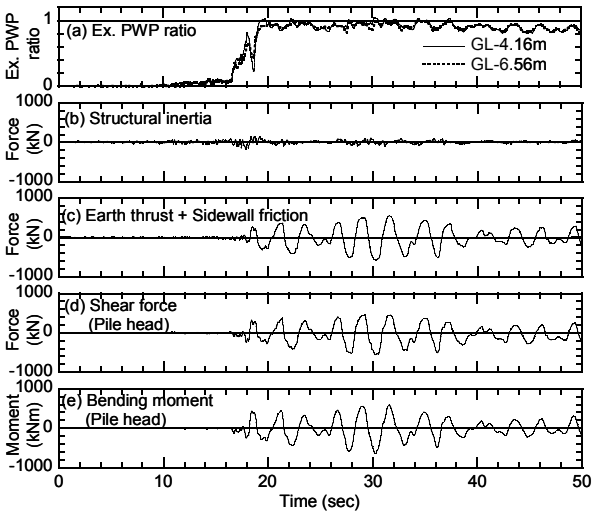

Figure 3. Excess pore water pressure ratio, structural inertia, resultant force of earth pressure and sidewall friction, shear force and bending moment at pile head (Case 3)

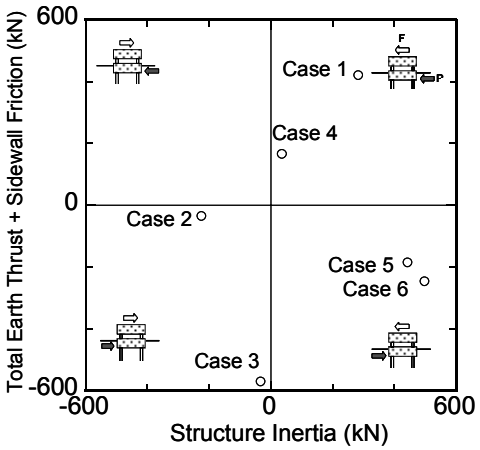

Figure 4. Relation between structure inertia and resultant force of total earth pressure and sidewall friction

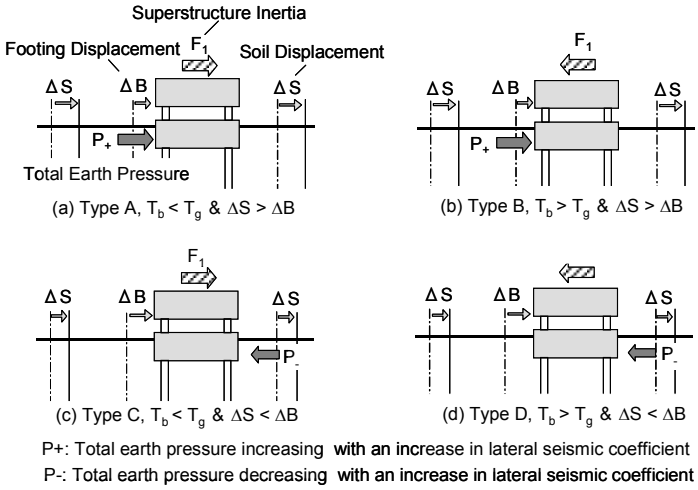

Figure 5. Phase difference between total earth pressure and superstructure inertia (After Tamura et al. 2005)

and sidewall friction when the bending moment at the pile head was maximum for Cases 1–6. Data shown in the first and third quadrants, and in the second and fourth quadrants respectively show that the structure inertia and the resultant force were in phase and out of phase by 180 deg. The structure inertia and the resultant force of the earth pressure and the sidewall friction were in phase for Cases 1–4 because the natural period of the superstructure was shorter than the predominant period of the soil and the displacement of the loose sand was greater than the footing displacement, corresponding to Type A in Fig. 5. Conversely, the structure inertia and the resultant force were out of phase by 180 deg for Cases 5 and 6 because the natural period of the superstructure was shorter than the predominant period of the soil and the displacement of the dense sand was smaller than the footing displacement, corresponding to Type C in Fig. 5.

4. EARTH PRESSURE AND SIDEWALL FRICTION

4.1 Measured Earth Pressure and Sidewall Friction

Figures 6 and 7 respectively present the relative displacement between the footing and the soil in addi-

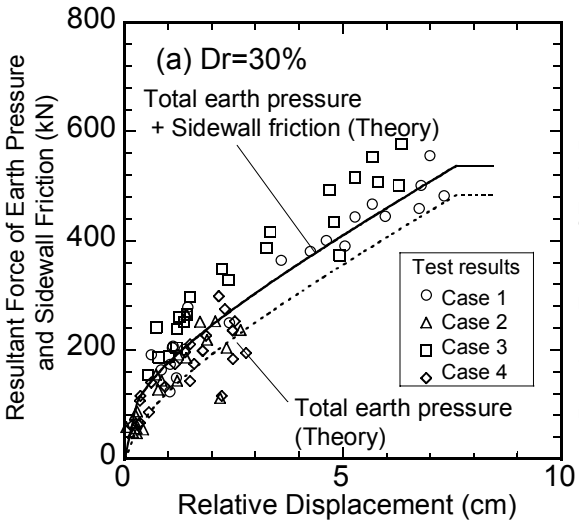

Figure 6. Relation between relative displacement and resultant force of total earth pressure and sidewall friction (Cases 1-4)

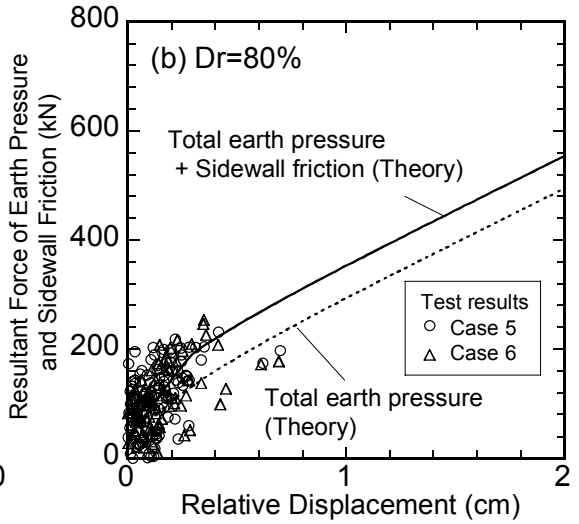

Figure 7. Relation between relative displacement and resultant force of total earth pressure and sidewall friction (Cases 5, 6)

tion to the resultant force peaks of the earth pressure and the sidewall friction for Cases 1–4 (D_r=30%) and Cases 5 and 6 (D_r=80%). The resultant force peaks increase concomitantly with increasing relative displacement for all cases. The resultant force peaks in Cases 1 and 3 (high stiffness piles), tend to be greater than those in Cases 2 and 4 (low stiffness piles) because the relative displacement peaks in Cases 1 and 3 were apt to be larger than those in Cases 2 and 4, which indicates that the pile bending stiffness affects the resultant force amplitude significantly in the loose sand case. The resultant force peaks in Case 5 (high stiffness piles) and Case 6 (low stiffness piles) were almost identical, indicating that the pile bending stiffness did not affect the resultant force amplitude in the dense sand case. The relative displacements in Cases 5 and 6, which were less than 1 cm, were much smaller than those in Cases 1–4. Consequently, the resultant force peaks in Cases 5 and 6 were much smaller than those in Cases 1–4 in spite of the dense sand model.

4.2 Estimated Earth Pressure and Sidewall Friction

The total earth pressure acting on an embedded footing, P_E is estimated as

$$P_E = P_{EL} - P_{ER} = \frac{1}{2}\gamma H^2 B(K_{EL} - K_{ER}) \tag{4.1}$$

in which P_{EL} and P_{ER} respectively signify the left and right side earth pressure, γ denotes the soil's unit weight, H represents the embedment depth of the footing, B stands for the passive and active side widths of the footing, and K_{EL} and K_{ER} respectively represent the seismic earth pressure coefficients of the footing's left and right sides proposed by Zhang et al. (1998). The seismic earth pressure depends not only on a seismic coefficient but also on the relative displacement between the footing and the soil in the free-field.

The sidewall friction P_F is estimated as

$$P_F = \mu P_0 D_{re} / D_{\max} \qquad (D_{re} \le D_{max}) \tag{4.2}$$

$$P_F = \mu P_0 \qquad (D_{re} > D_{max}) \tag{4.3}$$

$$P_0 = \frac{1}{2}\gamma H^2 L K_0 \tag{4.4}$$

in which μ denotes the friction coefficient between the soil and the footing's surface, P_0 is the earth pressure at rest, D_{re} signifies the relative displacement between the footing and the soil, D_{max} represents the relative displacement that the sidewall friction reaches its maximum, L stands for the length of the footing (shaking direction), and K_0 is the earth pressure coefficient at rest as estimated using Jaky's formula. Considering that the friction depends on the shear strength of the soil when the footing's surface is rough (Uesugi, 1986), the friction coefficient, μ is estimated as

$$\mu = \tan(\phi) \tag{4.5}$$

in which ϕ is the internal friction angle of the soil. The sidewall friction is assumed to be in phase with the total earth pressure.

To investigate the validity of the proposed method, the estimated total earth pressure was used, as shown in Figs. 6 and 7. The minimum relative displacement requiring development of the active state was assumed as 0.5% and 0.1% of the footing's embedment depth for Cases 1–4 (D_r=30%) and for Cases 5 and 6 (D_r=80%), respectively, based on results of previous studies (Zhang et al., 1998). The minimum relative displacement demanded development of the passive state, respectively as 4% and 1% of the footing's embedment depth for Cases 1–4 (D_r=30%) and Cases 5 and 6 (D_r=80%) (Fang et al., 2002). The respective internal friction angles for Cases 1–4 (D_r=30%) and for Cases 5 and 6 (D_r=80%) were 34 deg and 42 deg. The wall friction angle between the soil and footing was assumed to be half of the internal friction angle. The horizontal equivalent seismic coefficient was assumed as 0.2 for all cases. The minimum relative displacement at which the sidewall friction reaches its maximum was assumed to be 3 mm based on results of previous studies (Tamura et al., 2007). The estimated resultant force of the earth pressure and sidewall friction shows good agreement with the test results, indicating that the pro-

posed method can simulate the amplitude of the resultant force. The broken line in the figures shows the estimated total earth pressure (without the sidewall friction). The total earth pressure is dominant in the resultant forces but the estimated resultant forces (with the sidewall friction) show better agreement with the observed data.

5. RESPONSE DISPLACEMENT METHOD CONSIDERING EARTH PRESSURE AND SIDEWALL FRICTION

5.1 Analysis model for pile considering embedment effects

Figure 8 presents the proposed model with the response displacement method considering the earth pressure and sidewall friction. The earth pressure and sidewall friction acting on an embedded footing can be evaluated using the nonlinear spring between the footing and the free-field soil. The spring was evaluated using Eqs. (4.1)–(4.5). To incorporate consideration of the degree of fixation at pile head and pile tip, rotation springs, 1.41×10^5 kNm/rad for the high stiffness pile model and 1.65×10^5 kNm/rad for the low stiffness pile model, were set up the pile head and pile tip. The rotation springs were evaluated by the relation between the footing displacement and the horizontal load acting on the footing based on static horizontal loading tests without soil. The subgrade reactions acting on a pile were evaluated using a nonlinear spring based on the recommendations for design of building foundations in Japan (AIJ, 2001). The subgrade reactions were calculated using the *N*-value estimated by the shear wave velocity of soil, which were evaluated by the natural period of the soil model during slight shaking. The structure inertial force and the soil deformation were applied simultaneously to the pile-footing model. The pile stress was calculated using an incremental method.

5.2 Estimated Earth Pressure and Sidewall Friction

Figure 9 displays the relation between the estimated and observed resultant force of the total earth pressure and the sidewall friction per pile for all cases when the bending moment at the pile head reached its maximum. The respective positive and negative resultant forces show that the resultant force is in phase and out of phase by 180 deg with the inertia force. The observed inertial forces of the superstructure and footing, the soil displacement when the bending moment reached the maximum were used to estimate the pile stress. The reduction coefficients on liquefaction of the horizontal subgrade reaction coefficient, α and the ultimate subgrade reaction, β were assumed to be 0.01, 0.1 and 0.2. The estimated resultant force depends on the value of α and β because the subgrade reaction affects the footing displacement. The estimated resultant forces with $\alpha=\beta=0.2$ shows fairly good agreement with the experimentally obtained results, not only in terms of the amplitude but also in terms of the phase difference between the resultant forces and the structural inertia. The resultant forces were in phase with

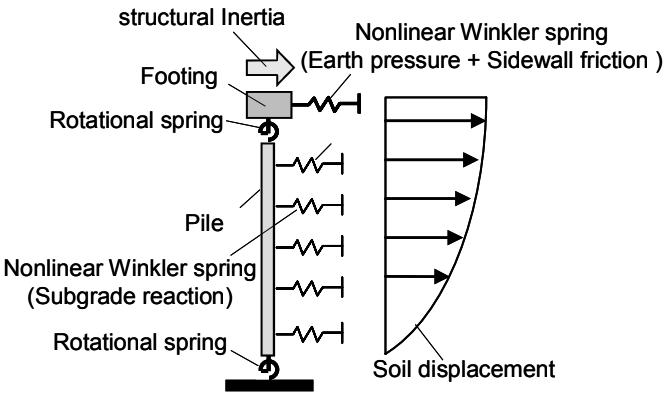

Figure 8. Analysis model for pile considering embedment effects

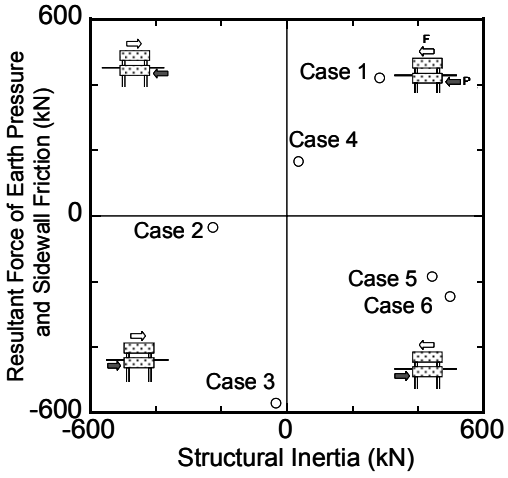

Figure 9. Estimated and observed resultant force of total earth pressure and sidewall friction

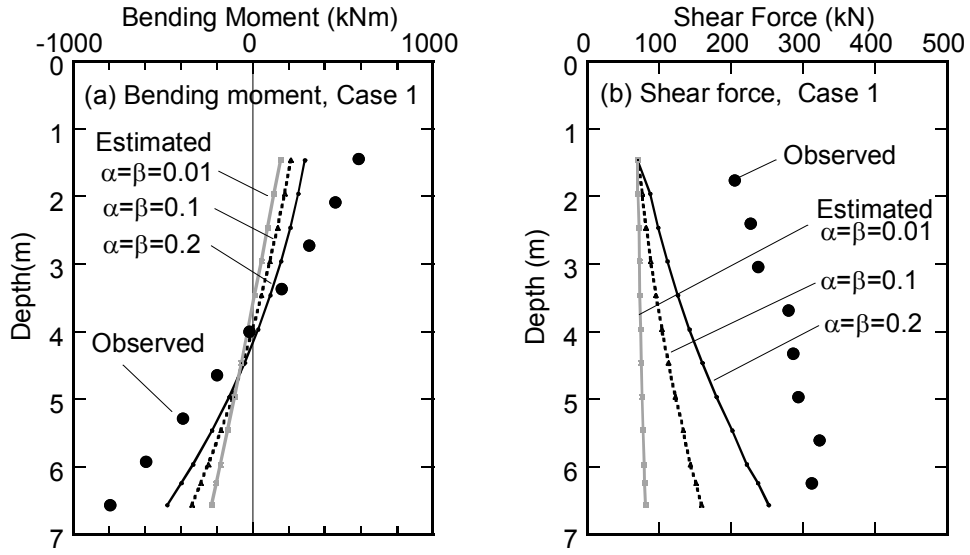

Figure 10. Estimated bending moment and shear force of pile without embedment effects and observed data (Case 1)

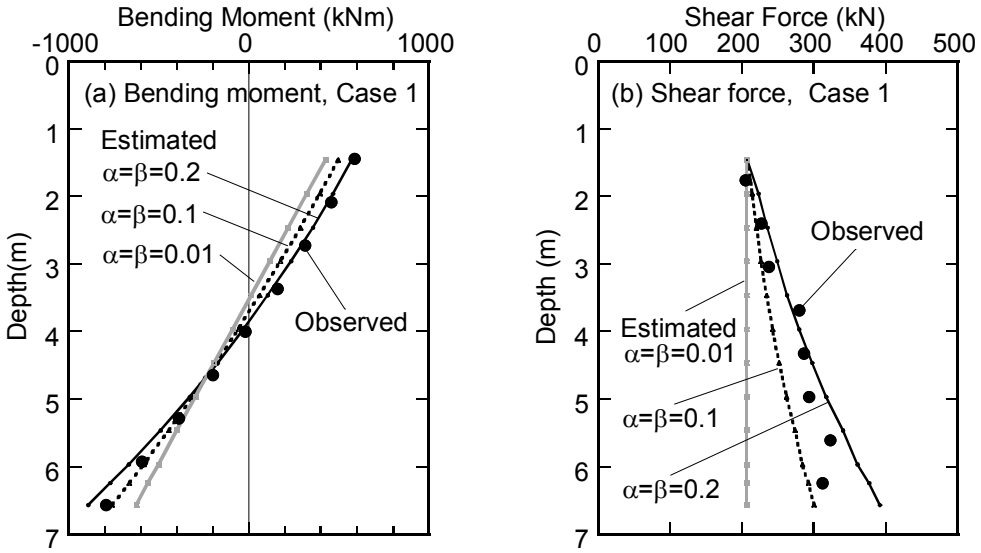

Figure 11. Estimated bending moment and shear force of pile with embedment effects and observed data (Case 1)

the structural inertia for Cases 1–4 and were out of phase by 180 deg with the structural inertia for Cases 5 and 6.

5.3 Estimated bending moment and shear force of piles

Figure 10 displays the vertical distribution of observed and estimated bending moments and shear forces of the pile in Case 1 when the bending moment at the pile head reached its maximum. The embedment effects, earth pressure and sidewall friction acting on the footing, were neglected. The reduction coefficients on liquefaction, α and β, were also assumed as 0.01, 0.1 and 0.2. The estimated bending moment and shear amplitudes were much smaller than the test results in every case, which suggests that the pile stress cannot be estimated accurately without the embedment effects.

Figure 11 shows the vertical distribution of estimated bending moment and shear force of the pile in Case 1, of which the embedment effects were considered. The estimated bending moments show fairly

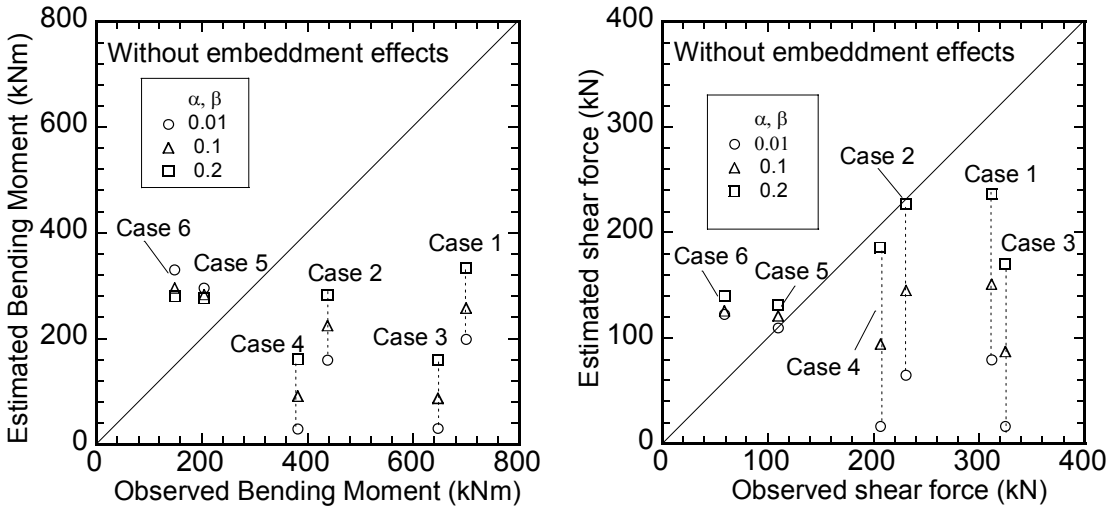

Figure 12. Estimated bending moment at pile head and shear force at pile tip without embedment effects and observed data (Cases 1-6)

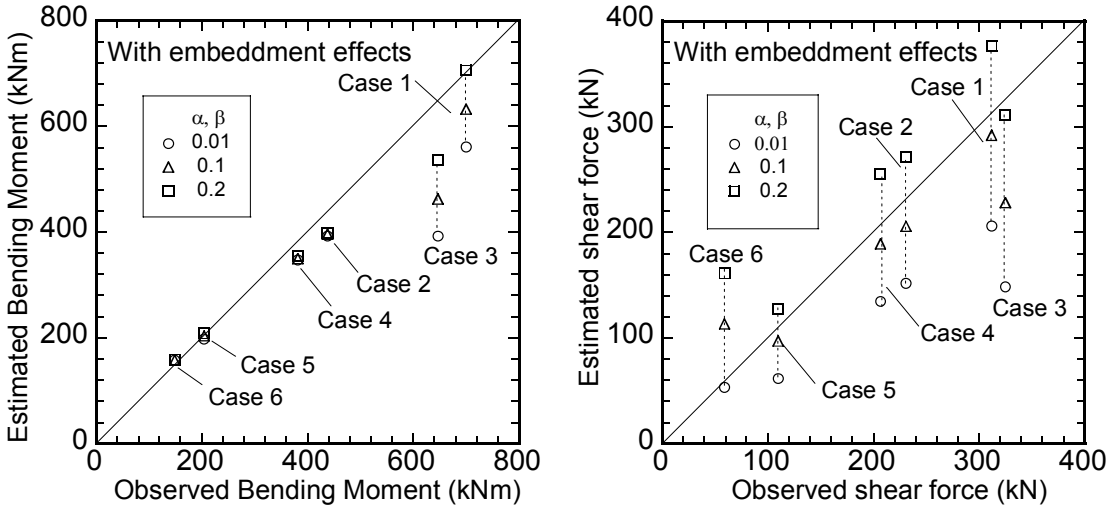

Figure 13. Estimated bending moment at pile head and shear force at pile tip with embedment effects and observed data (Cases 1-6)

good agreement with the observed data when α, β=0.1 and 0.2. The estimated bending moment amplitude with α, β=0.01 was smaller than the observed data. The observed pile shear force increased concomitantly with increasing depth, indicating that the soil acted on the pile as external pressure. This phenomenon was caused by the soil, for which the displacement was greater than the pile. The estimated pile shear forces also increased concomitantly with increasing depth and showed good agreement with the observed data when α, β=0.1 and 0.2. Estimated shear force with α, β=0.01 of which the variation was slight, agreed with the observed data at the pile head, but it was much smaller than the observed data at the pile tip.

Figure 12 display the relation between estimated bending moment at the pile head and shear force at the pile tip without embedment effects vs. observed data in Cases 1–6. The estimated bending moments with any α or β were smaller than the observed data in Cases 1–4. The resultant forces of the earth pressure and the sidewall friction acted on the footing as the external force in addition to the structural inertia, as portrayed in Fig. 4. Therefore, the bending moments without the embedment effects were underestimated. In contrast, the estimated bending moments with any α or β were larger than observed data in Cases 5 and 6. The resultant force of the earth pressure and the sidewall friction acted on the footing as the reaction force to the structural inertia in Cases 5 and 6, as portrayed in Fig.

4. Consequently, the estimated bending moment without the embedment effects were overestimated. The estimated shear forces at the pile tip with α, β =0.2 in all cases apparently show good agreement with the observed data. However, the estimated shear force did not correspond to the test results at the pile head, as presented in Fig. 10(b).

Figure 13 presents the estimated bending moment at the pile head and shear force at the pile tip with embedment effects and observed data. The estimated bending moments with any α or β show fairly good agreement with the observed data in Cases 2, and 4–6. The estimated bending moments with α, β =0.2 also show good agreement with the observed data in Cases 1 and 3. The effects of α, β on the estimated bending moment were small. However, the shear force at the pile tip depended significantly on α and β. The estimated shear forces with α, β=0.1, 0.2 agreed with the observed data. However, the estimated shear forces with α, β=0.01 were less than the observed data. To estimate the shear force at the pile tip, not only the embedment effects but also accurate subgrade reaction coefficients are necessary.

6. CONCLUSION

A response displacement method was developed with the earth pressure and sidewall friction acting on an embedded footing. Dynamic centrifuge tests on a superstructure-footing model that was supported by 2×2 piles in a sand deposit, a dry sand layer on liquefied soil, were conducted to verify the effectiveness of the proposed method. The earth pressure and sidewall friction were measured directly using small load cells set up on the embedded footing. The following conclusions were drawn.

(1) Centrifuge test results showed that the amplitudes of the resultant force of the earth pressure and sidewall friction depend on the pile rigidity and the relative soil density model. The measured resultant force of earth pressure and sidewall friction was in phase with the structure inertia force in case of the soil model with D_r=30%. In contrast, the measured resultant force was out of phase by 180 deg with the structure inertia force for the soil model with D_r=80%.

(2) Estimated amplitudes of the resultant force and the estimated phase difference between the resultant force and the structure inertia force showed good agreement with the experimentally obtained results, indicating that the proposed method can estimate the earth pressure and sidewall friction acting on an embedded footing considering the pile's bending stiffness and the relative soil density.

(3) Estimated amplitudes of the bending moment at pile head and the shear force at the pile tip agreed well with the observed results. The effects of subgrade reaction coefficients on the estimated bending moment at the pile head were small. In contrast, the subgrade reaction coefficients had significant effects on the estimated shear force at the pile tip. To estimate the shear force at the pile tip, not only the embedment effects but also accurate subgrade reaction coefficients are necessary.

REFERENCES

Fang, Y. S., Ho, Y. C. and Chen, T. J. (2002). Passive earth pressure with critical state concept. Journal of Geotechnical Engineering, ASCE, Vol. 128, No. 8, pp. 651–659.

Fujii, S., Isemoto, N., Satou, Y., Kaneko, O., Funahara, H., Arai, T. and Tokimatsu, K. (1998). Investigation and analysis of a pile foundation damaged by liquefaction during the 1995 Hyogoken-Nambu earthquake. Soils and Foundations – Special issue on Geotechnical Aspects of the 1995 Hyogoken Nambu Earthquake, No. 2, pp. 179–192.

Gadre, A. and Dobry, R. (1998). Lateral cyclic loading centrifuge tests on square embedded footing. Journal of Geotechnical and Geoenvironmental Engineering, ASCE, Vol. 124, No. 11, pp. 1128–1138.

Sugimura, Y. and Hirade, T. (1984). Experimental study of reduction effect of horizontal force due to embedment of the foundation. Summaries of Technical Papers of Annual Meeting, AIJ, Structures II, pp. 2409–2410. (in Japanese)

Tamura, S. and Tokimatsu, K. (2005). Seismic earth pressure acting on embedded footing based on large-scale shaking table tests. Geotechnical Special Publication, No. 145, ASCE, 2005, pp. 83–96.
Tamura, S., Imayoshi, T. and Sakamoto, T. (2007). Earth pressure and sidewall friction acting on an embedded footing in dry sand based on centrifuge tests. Soils and Foundations, Japan Geotechnical Society, Vol. 47, No. 4, pp. 811–819.
Uesugi, M. and Kishida, H. (1986). Influential factors of friction between steel and dry sands. Soils and Foundations, Vol. 26, No. 2, pp. 33–46.
Zhang, Jian-Min, Shamoto, Y. and Tokimatsu, K. (1998). Evaluation of earth pressure under any lateral deformation. Soils and Foundations, Japan Geotechnical Society, Vol. 38, No. 1, pp. 15–33.